Eur. Phys. J. Appl. Phys. **97**, 75 (2022)

https://doi.org/10.1051/epjap/2022220088

THE EUROPEAN PHYSICAL JOURNAL APPLIED PHYSICS

Regular Article

Examples of SVD decomposition contributions to the non-destructive testing of cultural heritage mural paintings using stimulated infrared thermography

Jean Luc Bodnar[1,*], Kamel Mouhoubi[1], and Jean Marc Vallet[2]

[1] URCA/GRESPI/CATHERM, UFR Sciences Exactes et Naturelles, BP 1039, 51687 Reims cedex 02, France
[2] CICRP, 21 rue Guibal, 13003 Marseille, France

Received: 28 March 2022 / Received in final form: 12 August 2022 / Accepted: 24 August 2022

Abstract. Stimulated infrared thermography has already shown its usefulness concerning heritage mural paintings conservation. However, the different pigments of the pictorial layer can, in certain unfavorable cases, lead to artefacts detection. Moreover, the fragility of these works of art requires the least invasive analyzes as possible. In the work presented here, we show, using theoretical and experimental studies, that the association of an SVD analysis with stimulated infrared thermography, seems to allow on the one hand, a notable reduction of this disturbing optical effect and we show on the other hand, that it seems to allow an early detection of these defects and therefore a lower energy deposit on studied works of art.

1 Introduction

Concerning heritage mural painting conservation, stimulated infrared thermography has already shown its usefulness [1–21].

The advantages of this control technique are as follows: It is non-destructive. It allows remote and contactless analysis. It may only request access to one side of the sample. It is easily customizable according to needs. It can be used on many types of samples. It is easy to use. It can be very fast. Finally, it allows the study of the first 100 micrometers of materials. Thus, it allows for example, the detection of delamination without physical contact as with the “finger tapping” analysis. It does not implement intense electromagnetic radiation as with X-ray radiography analysis. It is therefore complementary to the techniques already widely used in artworks conservation.

However, the different pigments of the pictorial layer can, in certain unfavourable cases, lead to artefacts detection.

Indeed, the defect detection principle, like a delamination, lies in the thermal barrier effect induced by the latter. For this, the studied sample is excited at the surface. The heat thus supplied then diffuses throughout the volume of the sample. This diffusion is uniform if the sample is healthy. This diffusion is disturbed if the sample contains a delamination which disturbs the internal thermal diffusion fluxes. This is what allows fault detection. The reading of the results will be quite simple if the surface excitation is homogeneous as in the case of a mono colour pictorial layer. If the paint layer is multi-coloured, the energy deposited depends on the colour of the paint layer pigments. The diffusion of heat then becomes more complex, as does the interpretation of the infrared thermograms obtained.

Moreover, a second limitation of the photothermal method is the fragility of the works of art studied. They require the least energetic analyzes possible.

In this research, we seek to reduce these two disadvantages.

With this objective, in this research, we associated an SVD type analysis (Singular Value Decomposition [22]) with stimulated infrared thermography. Indeed, we believe on the one hand, that the disturbing effects due to the optical effects induced by the pictorial layer are rather of high energy intensity (in the sense of signal processing) while those due to the presence of defects are rather more low energy intensity. Therefore, we believe that the higher EOF (Empirical Orthogonal Function), resulting from an SVD-type post-processing, will reduce the optical disturbance effect. We believe, on the other hand, that the integration properties of the SVD decomposition will allow an early detection of the defects present in the works of art studied and therefore less stressing of the latter.

In order to test these hypotheses, we worked in two stages: First, we developed a series of theoretical simulations. Then we developed a series of experiments. It is the approach followed and the results obtained in this context that we present here.

2 SVD decomposition principle

SVD decomposition is a classical and very powerful signal-processing tool [22]. It makes it possible to decompose a signal in the most suitable orthogonal base to the experimental device implemented to acquire it. So SVD

* e-mail: jean-luc.bodnar@univ-reims.fr

allows an experimental empirical model to be made since it is more natural, from the energy point of view, than the classical, Fourier or Laplace transforms. It is therefore of attractive use for non-destructive testing. This explains its implementation in this study.

SVD decomposition principle is as follows: first, an observational rectangular matrix X is made from the thermographic movie. X contains m lines and n columns, with $m > n$. m parameter corresponds to the pixels number (measuring point) of a thermogram; n parameter corresponds to the number of thermograms. X is built column-by-column. All pixel's values of one thermogram are regrouped in one column. That corresponds then to a measurement moment. The entire movie is scanned to build all the columns. Once this X observational matrix is built, its decomposition in singular values can start using the following equation (1):

$$X = U \cdot \Sigma \cdot V^T. \quad (1)$$

U is a square matrix with m lines and m columns. In this matrix, each column is orthogonal to the others. The columns represent the directions with the most important spatial energetic variation (with the meaning of the signal treatment) for the experience. These directions represent the axes of the empirical orthogonal basis of the experimentation. They are ranked in decreasing order of energetic importance. They are called "Empirical orthogonal function (EOF)". In this way, the first column of U matrix that is called EOF1 corresponds to the most energetic direction of the empirical model basis for the experimentation. Then, the second column of U matrix that is called EOF2, corresponds to the orthogonal direction which is energetically just below the previous one. This is done in the same way until the EOFm column.

Σ is a rectangular and diagonal matrix. It is composed of m lines and n columns. The diagonal values correspond to the representativeness of the previous "Empirical Orthogonal Function" (EOF). These values are ranked from the most energetic EOF to the least energetic EOF. In this way, the first value Σ_1 of Σ the matrix corresponds to the energetic representativeness of EOF_1. The second one (Σ_2, $\Sigma_2 < \Sigma_1$) corresponds to the energetic representativeness of EOF_2. This logical reasoning is reproduced until Σ_m value.

V is a square matrix with n lines and n columns. Each column is perpendicular to the others. The columns represent the direction of the most important temporal energetic variations of the experiment. V is not homogeneous to a thermogram as U matrix. So it is more difficult to explain. Nevertheless, it could be interesting for defect depth characterization. It has not been studied here.

In this study, we used the SVD decomposition properties on the one hand, to reduce the disturbing effect of the pictorial layer and on the other hand to allow early detection of the defects.

In the first case, we believe that the photothermal variations due to the presence of defects are, from an energy point of view (in the sense of signal processing), less important than those due to the inhomogeneity of energy deposition.

Indeed, the radiative flux emitted and collected by the infrared thermography camera depends on the one hand on the radiative properties of the sample studied. It also depends on the thermal contrast induced by the presence of the defect. In the first case, the variations can vary from simple to tenfold (absorptivity less than 0.1 for a gold coating and absorptivity close to 1 for a black paint layer). This is what generates the disturbing effect of the pictorial layer. In the second case, the variations are linked to the thermal barrier effect due to the presence of a defect. In order not to damage the work of art, this effect is limited to a few degrees, i.e. for a temperature close to ambient (300 K) at variations of less than 1%. As indicated previously, these variations are therefore potentially much lower than those generated by the colorimetric inhomogeneity's of the pictorial layer.

Therefore, the very first EOFs of the SVD decomposition should reveal this inhomogeneity of energy deposit.

The following EOFs would be less sensitive to it and would rather reveal the photothermal signature of the defects. Thus, to study the photothermal signatures related to the defect, we propose to eliminate the very first EOFs, the most energetic ones and to work only on the following EOFs (within the limit of those presenting a good signal/noise ratio).

In the second case, we believe that the global analysis of a series of thermograms offered by the SVD decomposition will allow an integration of information and therefore an earlier detection of defects than the direct analysis of raw thermograms.

3 Theoretical study

To test our approach, first a set of simulations were developed. They implemented the finite element analysis to model the photothermal experiment associated to the study.

The analyzed sample is a block of plaster, which has thermophysical properties closed to a real wall painting. Its geometrical dimensions are 160 mm in length, 120 mm in width and 20 mm in thickness. Its thermophysical properties are of a thermal conductivity equal to 0.4 W/mK, a density equal to 1100 kg/m^3 and a heat capacity equal to 830 J/kg K. The thermal diffusivity is then equal to 4.38×10^{-7} m^{-2}/s.

To simulate delamination, six air layers have been studied in this sample. They have a parallelepiped form. They have the same geometrical dimensions. Their length and width are equal to 20 mm. Their thickness is equal to 4 mm. Their depth varies from 2 to 12 mm with 2 mm spacing.

The first defect is located at the top left of the sample. Its depth is equal to 2 mm. The second defect is in the bottom left of the sample. Its depth is equal to 4 mm. The third defect is located on the top middle of the sample. Its depth is equal to 6 mm in depth. The fourth defect is in the bottom middle of the sample. Its depth is equal to 8 mm. The fifth defect is located on the top right of the sample. Its depth is equal to 10 mm. The last defect is in the bottom right of the sample. Its depth is equal to 12 mm (Figs. 1 and 2).

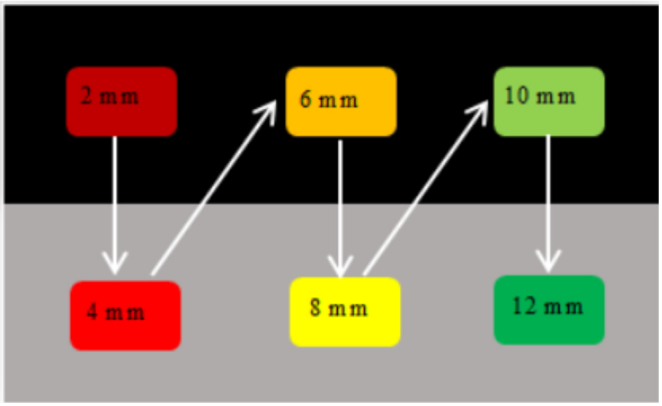

Fig. 1. The theoretically studied sample (top view).

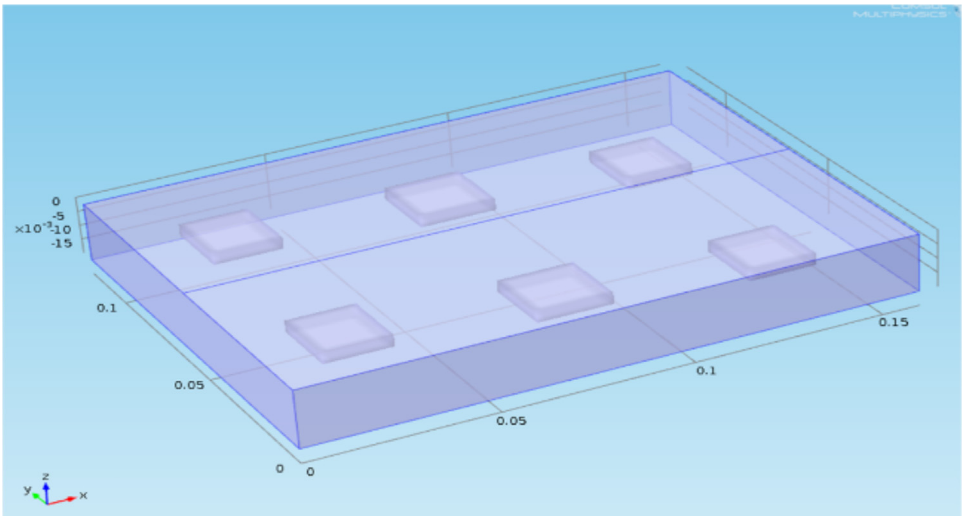

Fig. 2. The theoretically studied sample (side view).

The thermophysical properties of these defects are those of the air at 20 °C. The thermal conductivity is equal to 0.026 W/mK. The density is equal to 1.17 kg/m^3. The heat capacity is equal to 1006 J/kg K. The thermal diffusivity is then equal to 2.22×10^{-5} m^2/s.

Lastly, the sample has been divided in two parts to simulate the optical effects of the pictorial layer. The first one covers the defects that are located at 4 mm, 8 mm and 12 mm in depth. The second one covers the defects that are located at 2 mm, 6 mm, and 10 mm in depth. Furthermore, the imposed flux was energetically 1.5 times more on the second part than on the first one.

The excitation signal is a crenel. Its duration is equal to 2 s. The analysis time is equal to 200 s. The acquisition frequency is equal to 1 Hz. The deposited energy is equal to 1500 W. Finally, we have considered a model with no loss.

The raw thermograms obtained at $t = 3$ s, $t = 8$ s, $t = 13$ s, $t = 28$ s, $t = 53$ s, $t = 91$ s, $t = 177$ s and $t = 200$ s are presented in Figure 3. The thermograms show, as expected, a more important photothermal signature located at the place of the defects. They show also that the deeper the defect is, the later the signatures appear. Lastly, they show, as expected, that these signatures are affected by the inhomogeneous energy deposit.

The obtained results after a SVD decomposition are presented in Figure 4. This decomposition has been calculated considering the first 190 seconds of the cooling phase of the sample (from $t = 3$ s to $t = 193$ s). Figure 4 presents the nine first EOF from the SVD decomposition. First, theses synthetics thermograms allow, as expected, the detection of the six defects. Figure 4 also shows, as expected, that the first EOF (1 and 2) are more sensitive to the inhomogeneous energy deposit. It shows then that the following EOF seem to be less sensitive to this inhomogeneous energy deposit. This theoretical result really seems to confirm the advantage of a SVD post processing in improving the non-destructive testing of artwork.

In Figure 5, we present the first EOFs obtained after a SVD decomposition, calculated between $t = 3$ s (beginning of the cooling) and $t = 8$ s. It shows that EOF 5 seems to allow three defects detection. If we analyze the raw thermogram obtained at $t = 8$ s, we can detect only one

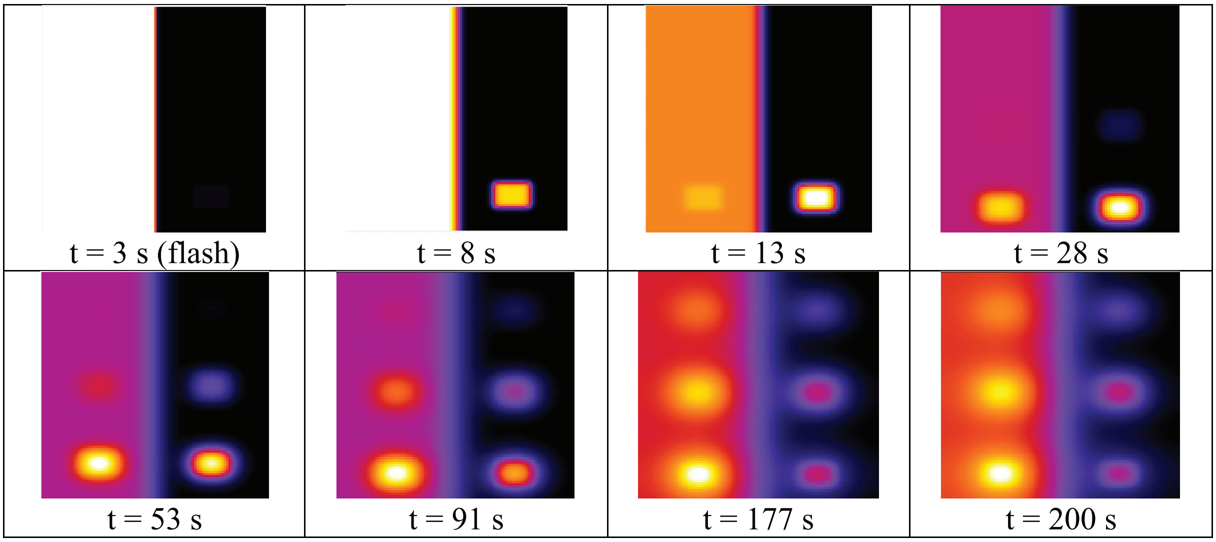

Fig. 3. Example of theoretical thermograms obtained ($t=3$ s, $t=8$ s, $t=13$ s, $t=28$ s, $t=53$ s, $t=91$ s, $t=177$ s and $t=200$ s).

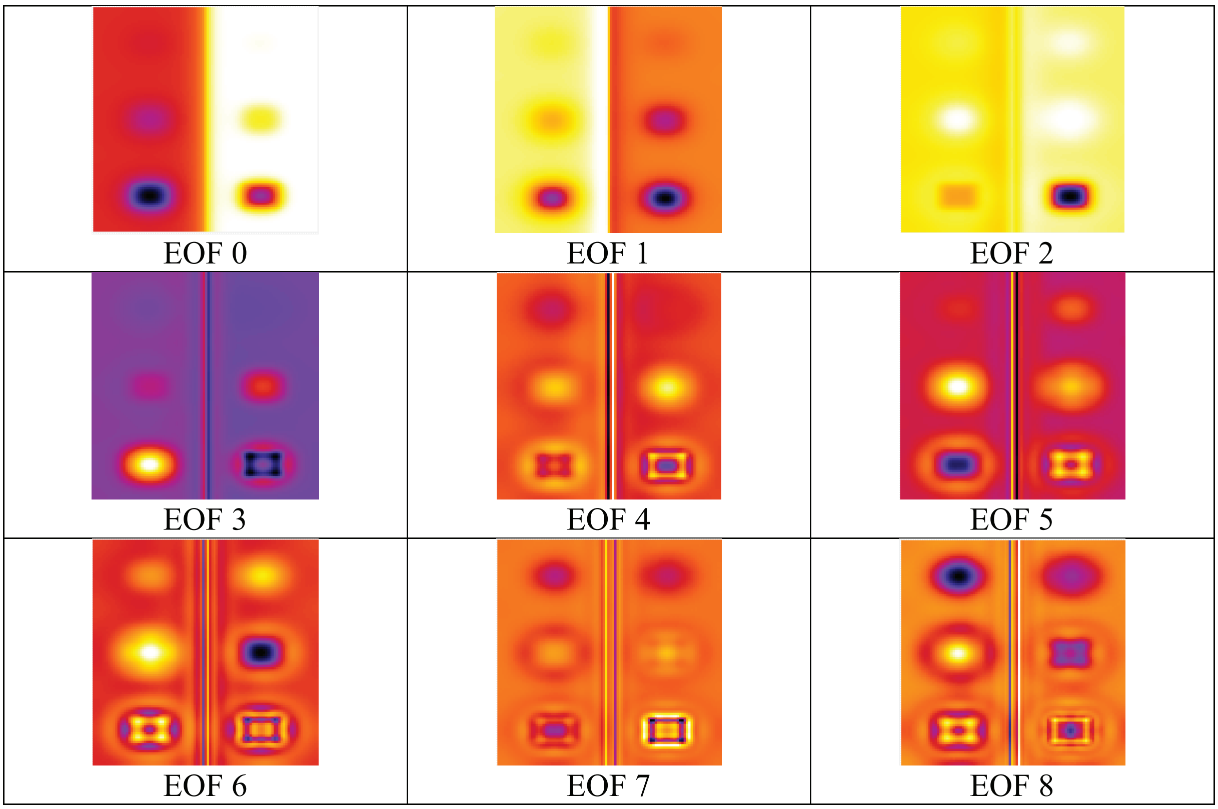

Fig. 4. The first 9 EOFs obtained (SVD decomposition between $t=3$ s and $t=193$ s).

defect. As the reduction of the optical effect is kept by the SVD decomposition, these results show, thanks to SVD post processing, possible reduction of the photothermal analyses duration. This implies a lower energy deposit during analyzes and thus better artwork conservation.

In Figure 6, we present the first EOFs obtained after an SVD decomposition calculated over a time range extending from $t=3$ s to $t=53$ s. Whereas, Figure 3 shows that for this duration of analysis, only the first four defects are detectable, Figure 6 shows that the mathematical post-processing seems to allow the detection of all the defects present in the analyzed sample. This theoretical result confirms the previous observation. It therefore confirms the interest of SVD decompositions in terms of early detection of defects (and reduction of disturbing effects of the pictorial layer).

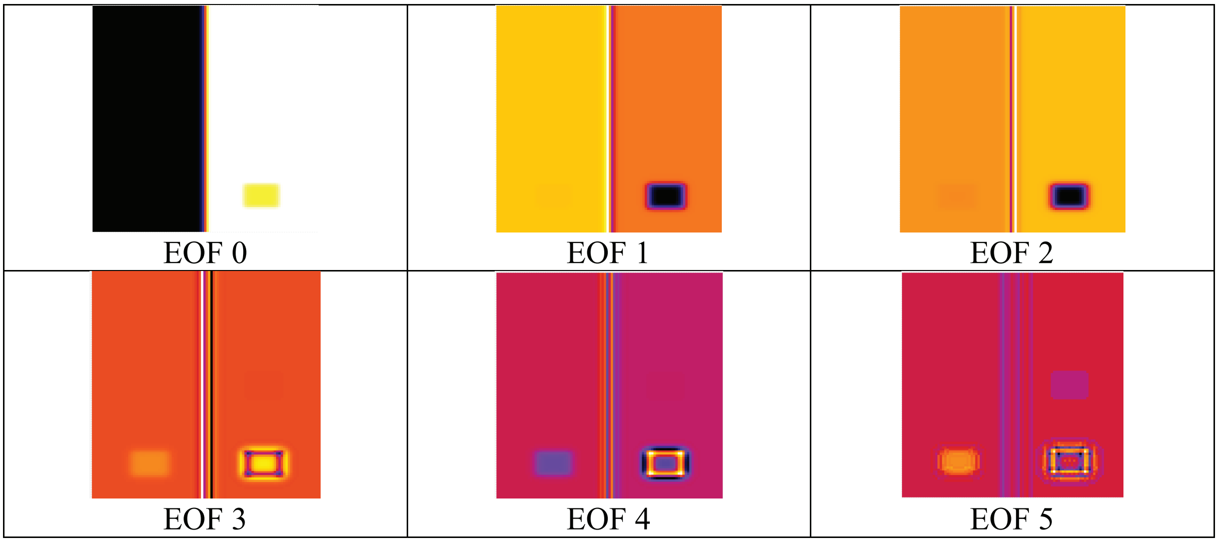

Fig. 5. The first 6 EOFs obtained (SVD decomposition between $t = 3$ s and $t = 8$ s).

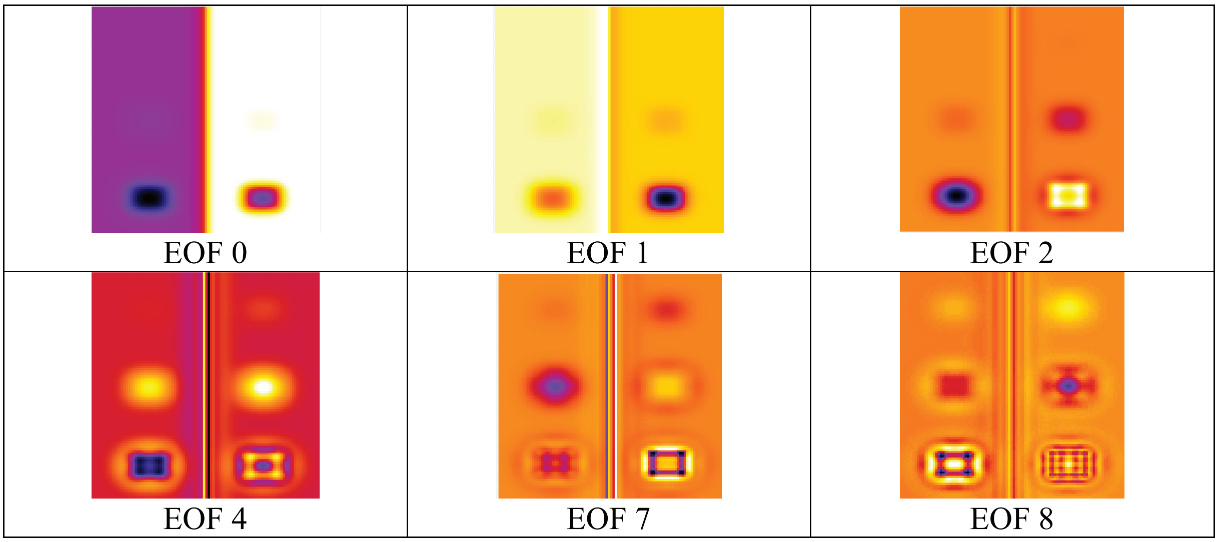

Fig. 6. The first 6 EOFs obtained (SVD decomposition between $t = 3$ s and $t = 53$ s).

4 Experimental studies

Following these encouraging theoretical results, we moved on to an experimental study of a partial copy of a mural painting from the cathedral of Angers. It was developed using the "thermoart" device. SVD-type post-processing was developed using the "irexplorer" software package. Let's now discover the work of art studied, the "thermoart" and "irexplorer" devices and finally the experimental results obtained.

4.1 The studied artwork: a partial copy of "Saint Maurille en Evêque" mural painting from the Angers cathedral (France)

The work of art studied is a partial copy of the mural painting "Saint Maurille en Evêque" in the cathedral of Angers (Fig. 7). It was carried out by Emilie Detalle, heritage restorer. It is shown in Figure 8. Its characteristics, provided by E. Detalle, are as follows: the support is made of a lime and sand mortar. Its dimensions are 15 cm square and 1.5 cm thick. The pictorial layer, produced in fresco, is made up of different pigments: vermilion, minium, lapis lazuli, yellow ochre, carbon black, lead white, malachite, and a gold leaf mix.

Detachments that can affect the wall painting were simulated by incorporating 5 extruded polystyrene inclusions of 30 mm in diameter and about 1 mm thick in the artwork. These defects are distributed over the sample and located at depths of 2 mm, 3 mm, 4 mm, 5 mm and 6 mm (Fig. 9).

4.2 The experimental device implemented for the study

The experimental device used for the study comprises two modules. The first is a data acquisition module. This is the "thermoart" device developed in the laboratory. On the one

Fig. 7. The mural painting studied.

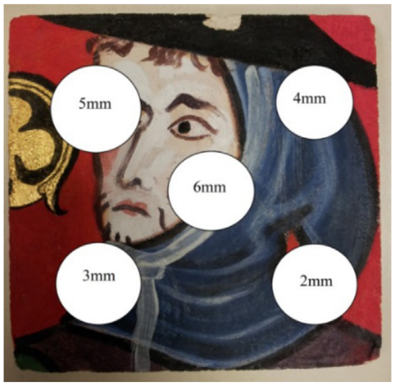

Fig. 9. Location of the defects inserted in the studied artwork.

Fig. 8. The mural painting "Saint Maurille en Evêque" decorates the Angers cathedral.

hand, it allows a controlled excitation of the analyzed sample. It also allows a synchronous acquisition of the photothermal response of the latter.

The second module is a data post-processing software package. This is the "irexplorer" software package. It allows to apply an SVD decomposition to the thermographic film obtained. The latter can be applied over a time range defined by the user. Finally, the software gives access to all the EOFs calculated after SVD decomposition (Fig. 10).

4.3 The experimental conditions selected for the study

The experimental conditions used for the study are the following.

The chosen infrared camera is the FLIR SC655. It is a bolometers camera. It presents a sufficient NETD and an acquisition frequency for the study, while keeping the cost reasonable.

The optics associated with this infrared camera is a 24.6 mm focal length lens. This choice makes it possible to obtain a wide analysis field, while maintaining a sufficiently resolved defect signature.

In order to limit radiative, environmental or atmospheric disturbances, this camera is placed perpendicular to the fresco studied. The distance between the two is equal to about 50 cm.

The exciting sources used for the study are two 500-Watt halogen lamps. They are placed on either side of the camera. The distance from the sample studied is equal to about 50 cm. They illuminate the latter with an angle of about 45 degrees counted along the horizontal axis (Fig. 11). This experimental configuration allows a uniform and sufficient illumination of the studied work of art.

The camera and light sources are controlled by the "thermoart" device. The chosen excitation signal is a crenel. Its duration is equal to 127 s. The total analysis time is equal to 375 s. The acquisition frequency is equal to 1 Hz. Finally, the excitation begins 11 seconds after the start of the thermographic acquisition.

4.4 The experimental results obtained

In Figure 12, we present the raw thermograms obtained at $t = 11$ s, $t = 17$ s, $t = 22$ s, $t = 26$ s, $t = 50$ s, $t = 75$ s, $t = 100$ s, $t = 116$ s, $t = 148$ s, $t = 175$ s, $t = 249$ s and $t = 350$ s. As theoretically expected, these raw thermograms show a larger photothermal signature directly above the defects. The signature of the three shallower defects is highly contrasted unlike the two deepest ones. Moreover, and as expected, the deeper the defect, the more its signature appears later. Lastly, these signatures are disturbed by the inhomogeneity of the energy deposit.

In Figure 13, we then present the results obtained after an SVD decomposition. The latter was calculated during the first 135 seconds of the sample studied cooling phase (from $t = 140$ s to $t = 275$ s). This figure presents the first three EOFs of the SVD decomposition. It first shows that these synthetic thermograms allow the detection of the five defects, in a clearer way than the raw thermograms. It then shows and as expected, that if the first two EOFs are sensitive to the energy deposition inhomogeneity, EOF2 seems to be much less sensitive to it. This experimental result seems to confirm the interest of an SVD treatment to improve the artworks non-destructive testing.

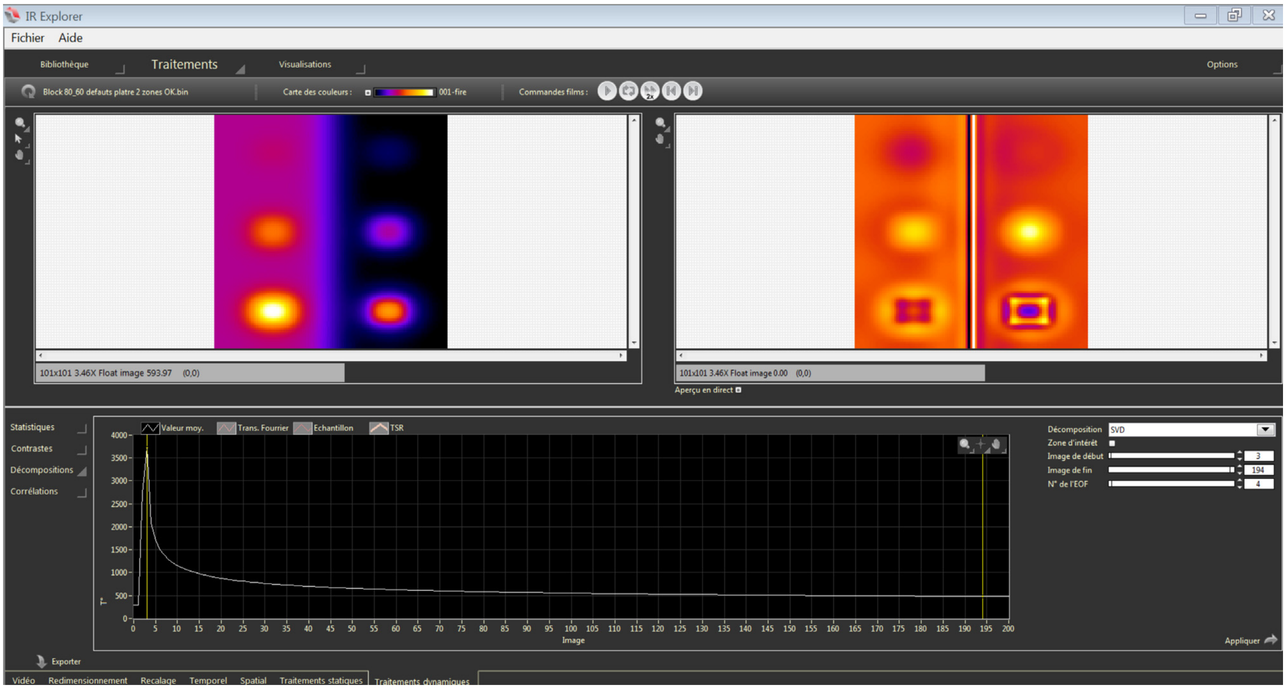

Fig. 10. Example of the control panel of the "irexplorer" software package obtained during the theoretical study.

Fig. 11. The wall painting studied during photothermal analysis.

In Figure 14, we then present the first EOFs obtained after an SVD decomposition calculated over a shorter and especially very early time range. The calculation time range extends from $t = 11$ s (start of excitation) to $t = 26$ s. Whereas, Figure 12 shows that for this duration of analysis only the shallowest defect is detectable, on reading the raw thermograms, Figure 14 shows that the SVD decomposition seems to allow (EOF3) the detection of the three first defects, while maintaining the reduction of the disturbing effects of the pictorial layer. This result seems to confirm the theoretical results. On the other hand, it seems to open the way to a possible reduction in the duration of photothermal analyzes while maintaining the reduction of the disturbing effects of the pictorial layer.

To confirm this very encouraging result, in Figure 15, we present the first EOFs obtained after an SVD decomposition calculated over a wider time range, extending from $t = 11$ s (start of excitation) to $t = 116$ s (end of excitation). Whereas Figure 12 shows that for this duration of analysis, only the first three defects are detectable on the raw thermograms, Figure 15 shows that the mathematical post-processing seems to allow the

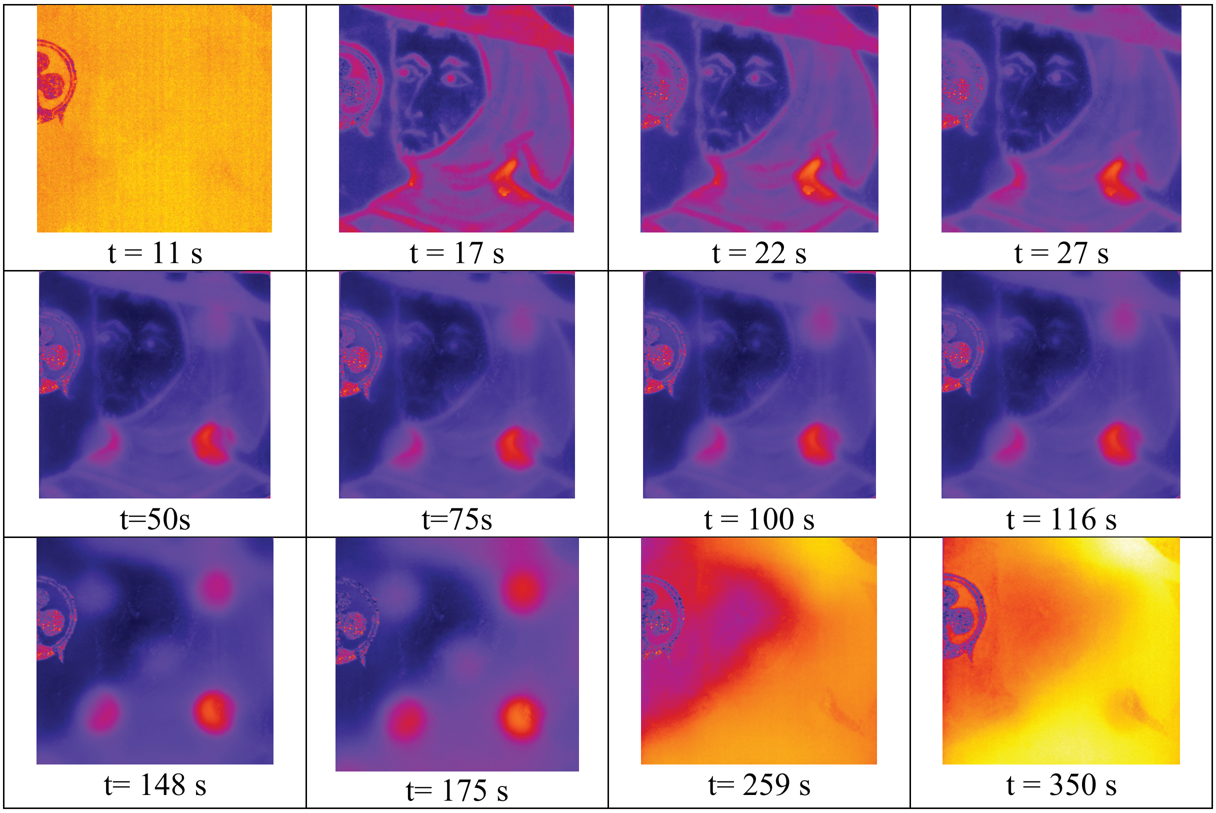

Fig. 12. Example of raw thermograms obtained.

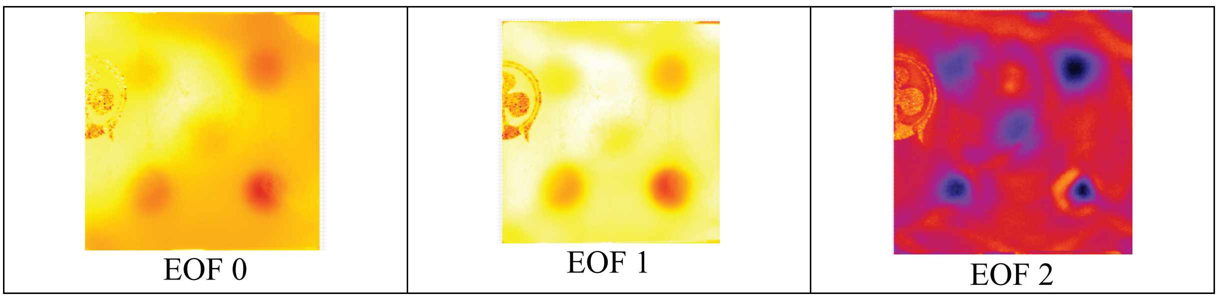

Fig. 13. The first 3 EOFs obtained (SVD decomposition between $t = 140\,\mathrm{s}$ and $t = 275\,\mathrm{s}$).

detection of all the faults present in the sample analyzed. This second experimental result confirms the interest of SVD decompositions in terms of early detection of defects and reduction of disturbing effects of the pictorial layer.

5 Conclusion

In this work, we have approached the contribution of an SVD decomposition to infrared thermography to improve the aid in the conservation of cultural heritage wall paintings.

We first recalled that if the non-destructive testing of these works of art by stimulated infrared thermography is already very efficient, it can be hampered on the one hand by the different colors of the pictorial layer. On the other hand, it can be hampered by too much stress.

We then presented the scientific basis of our approach. In the first case, our hypothesis consists in considering that the disturbances brought by an inhomogeneity of energy deposit are more important from an energy point of view (in the sense of signal processing) than those due to the presence of defects. During an SVD decomposition, the very first EOFs represent the most energetic fluctuations while the following EOFs represent the less and less energetic fluctuations. This means in our case, that the analysis of higher order EOFs should make it possible to partly overcome the inhomogeneity of energy deposition and rather to consider the variations of photothermal signals due to the presence of defects. In the second case, we believe that the global analysis of a series of thermograms offered by the SVD decomposition will allow an integration of information and therefore an earlier detection of defects than the direct analysis of raw thermograms.

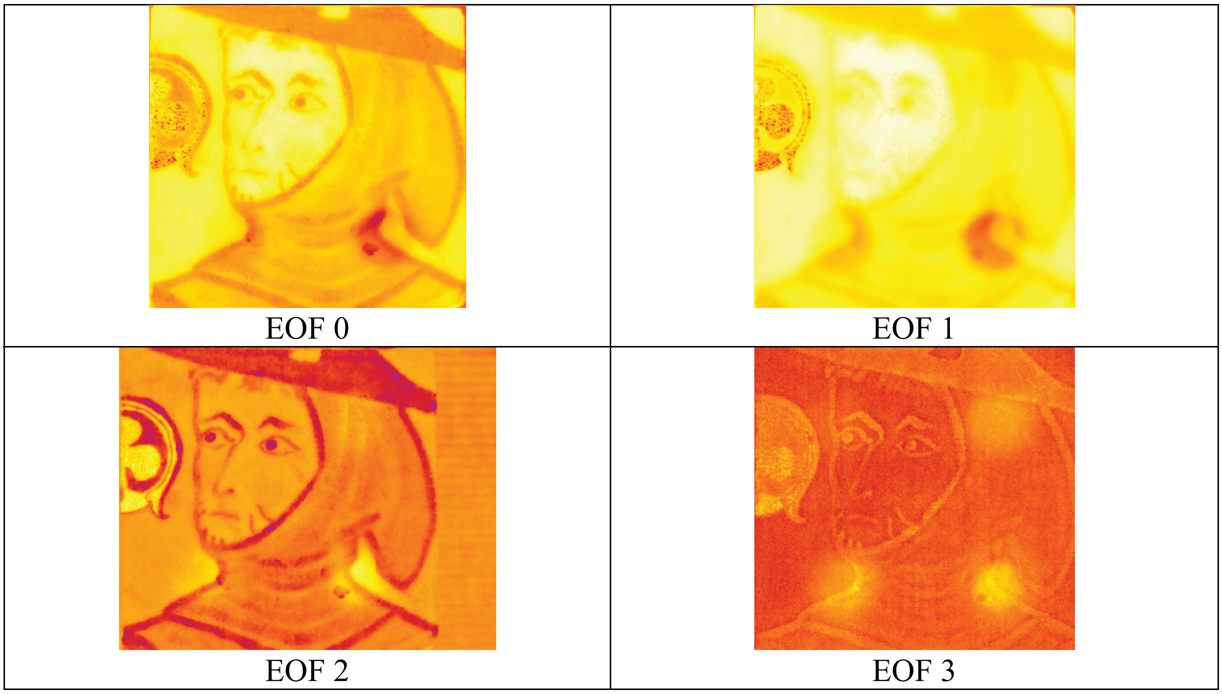

Fig. 14. The first 4 EOFs obtained during an SVD decomposition using a reduced time range from $t = 11$ s to $t = 26$ s.

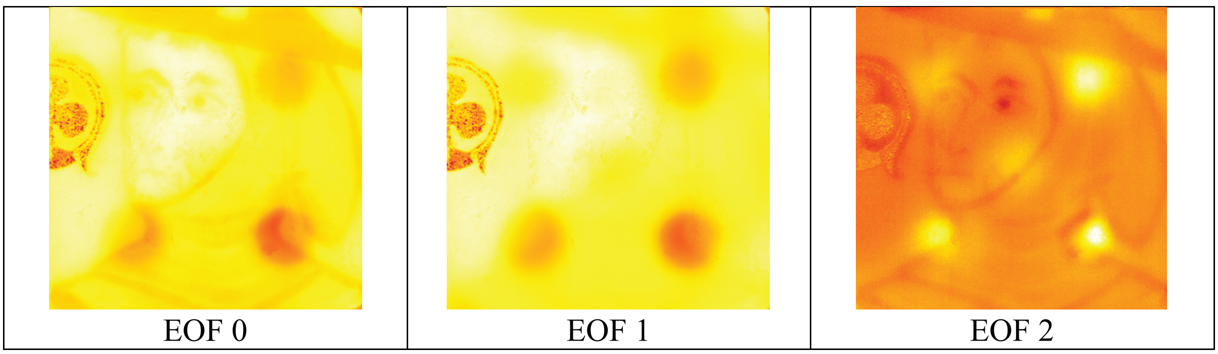

Fig. 15. The first 4 EOFs obtained during an SVD decomposition using a reduced time range from $t = 11$ s to $t = 116$ s.

To confirm these hypotheses, we then developed a theoretical study based on the modeling of the photothermal experience. We then showed on the one hand that the higher EOFs allow a better detection of the defects present in the work of art studied, because they significantly reduce the disturbing effects of the pictorial layer. We have shown on the other hand, that the SVD decomposition seems to allow an earlier detection of the defects than the raw thermograms.

Finally, we developed an experimental study to confirm the theoretical results obtained. We then showed during the study of a copy of a wall painting of the cathedral of Angers, that the higher order EOFs indeed allow the detection of the defects present in the sample analyzed while being much less sensitive to the optical effects induced by the different colors of the pictorial layer. Next we showed experimentally that an SVD decomposition seems to be able to allow earlier detection of defects than an analysis of raw thermograms, which would be a considerable asset for in situ analyses.

These very encouraging results seem to allow the improvement of non-destructive testing of works of art by stimulated infrared thermography. Moreover they now ask to be generalized. They also need to be confirmed during in situ analysis. Studies in this direction are in progress.

Author contribution statement

All authors contributed to the study conception and design. Material preparation, data collection and analysis were performed by all authors.

The first draft of the manuscript was written by J.L. Bodnar and all authors commented on previous versions of the manuscript. All authors read and approved the final manuscript.

References

1. M.F. Alberghina, G. Milazzo, S. Schiavone, L. Randazzo, M. Ricca, N. Rovella, F. Spatafora, E. Fiorenza, M.F. La Russa, The contribution of microchemical analyses and diagnostic imaging to the conservation and identification of the degraded surfaces of hellenistic-roman wall paintings from Solunto (Sicily), Stud. Conserv. **66**, 342 (2021)
2. P. Bison, A. Bortolin, G. Cadelano, G. Ferrarini, F. López, X. Maldague, Comparison of image processing techniques for the on-site evaluation of damaged frescoes, Proc. SPIE **9105**, 91050 (2014)
3. J.L. Bodnar, J.C. Candoré, J.L. Nicolas, G. Szatanik, V. Detalle, J.M. Vallet, Stimulated infrared thermography applied to help restoring mural paintings, NDT & E Int. **49**, 40 (2012)
4. J.-L. Bodnar, K. Mouhoubi, L.D. Pallo, V. Detalle, J.-M. Vallet, T. Duvaut, Contribution to the improvement of heritage mural painting non-destructive testing by stimulated infrared thermography, Eur. Phys. J. Appl. Phys. **64**, 11001 (2013)
5. G. Cadelano, P. Bison, A. Bortolin, G. Ferrarini, F. Peron, M. Girotto, M. Volinia, Monitoring of historical frescoes by timed infrared imaging analysis, Opto-Electr. Rev. **23**, 100 (2015)
6. J.C. Candoré, J.L. Bodnar, V. Detalle, P. Grossel, Non-destructive testing of works of art by stimulated infrared thermography, Eur. Phys. J. Appl. Phys. **57**, 21002 (2012)
7. G. Carlomagno, C. Meola, Comparison between thermographic techniques for frescoes NDT, NDT&E Int. **35**, 559 (2002)
8. C. Daffara, S. Parisotto, P.I. Mariotti, Mid-infrared thermal imaging for an effective mapping of surface materials and sub-surface detachments in mural paintings: integration of thermography and thermal quasi-reflectography, Proc. SPIE **9527**, 95270I (2015)
9. D. Gavrilov, E. Maeva, O. Grube, I. Vodyanoy, R. Maev, Experimental comparative study of the applicability of infrared techniques for non-destructive evaluation of paintings, J. Am. Inst. Conserv. **52**, 48 (2013)
10. E. Grinzato, P. Bison, S. Marinetti, V. Vavilov, Non-destructive evaluation of delaminations in fresco plaster using transient infrared thermography, Res. Nondestruct. Evaluat. **5**, 257 (1994)
11. S. Laureti, S. Sfarra, H. Malekmohammadi, P. Burrascano, D.A. Hutchins, L. Senni, G. Silipigni, X.P.V. Maldague, M. Ricci, The use of pulse-compression thermography for detecting defects in paintings, NDT&E Int. **98**, 147 (2018)
12. S. Laureti, C. Colantonio, P. Burrascano, M. Melis, G. Calabrò, H. Malekmohammadi, S. Sfarra, M. Ricci, C. Pelosi, Development of integrated innovative techniques for paintings examination: the case studies of The Resurrection of Christ attributed to Andrea Mantegna and the Crucifixion of Viterbo attributed to Michelangelo's workshop, J. Cultur. Heritage **40**, 1 (2019)
13. K. Mouhoubi, V. Detalle, J.-M. Vallet, J.-L. Bodnar, Improvement of the non-destructive testing of heritage mural paintings using stimulated infrared thermography and frequency image processing, J. Imag. **5**, 72 (2019)
14. K. Mouhoubi, K. Dieng, C. Fomena, H. Feddini, A. Salami, J.M. Vallet, J.L. Bodnar, Contribution to the improvement of the detection of defects located in heritage works of art by stimulated infrared thermography associated with a spatial reallocation of the colorimetric dynamics of the thermograms, in *QIRT 2020, 21–30 sept 2020, Porto, Portugal* (2020)
15. S. Sfarra, P. Huke, P. Theodorakeas, D. Paoletti, N.P. Avdeledis, D. Ambrosini, R. Klattenhoff, M. Koui, Non-destructive testing (NDT) methods used for the study of stone frescoes, in *NDT in Progress 2011-6th International Workshop of NDT Experts* (2011), pp. 295–304
16. S. Sfarra, C. Ibarra-Castanedo, D. Ambrosini, D. Paoletti, A. Bendada, X. Maldague, Non-destructive testing techniques to help the restoration of Frescoes, Arab. J. Sci. Eng. **39**, 3461 (2014)
17. S. Sfarra, P. Theodorakeas, C. Ibarra-Castanedo, N.P. Avdelidis, D. Ambrosini, E. Cheilakou, D. Paoletti, M. Koui, A. Bendada, X. Maldague, How to retrieve information inherent to old restorations made on frescoes of particular artistic value using infrared vision? Int. J. Thermophys. **36**, 3051 (2015)
18. M. Tortora, S. Sfarra, M. Chiarini, V. Daniele, G. Taglieri, G. Cerichelli, Non-destructive and micro-invasive testing techniques for characterizing materials, structures and restoration problems in mural paintings, Appl. Surf. Sci. **387**, 971 (2016)
19. V.P. Vavilov, E. Grintsato, P. Bizon, S. Marinetti, Thermal testing of air exfoliation under frescos, Defektoskopiya **7**, 73 (1994)
20. V. Vavilov, S. Marinetti, E. Grinzato, P.G. Bison, S. Dal Toè, D. Burleigh, Infrared thermographic nondestructive testing of frescos: thermal modeling and image processing of three-dimensional heat diffusion phenomena, Mater. Evaluat. **60**, 452 (2002)
21. J. Williams, F. Corvaro, J. Vignola, D. Turo, B. Marchetti, M. Vitali, Application of non-invasive active infrared thermography for delamination detection in fresco, Int. J. Thermal Sci. **171**, 107185 (2022)
22. I.T. Jolliffe, *Principal Component Analysis* (Springer, 2002)

Cite this article as: Jean Luc Bodnar, Kamel Mouhoubi, Jean Marc Vallet, Examples of SVD decomposition contributions to the non-destructive testing of cultural heritage mural paintings using stimulated infrared thermography, Eur. Phys. J. Appl. Phys. **97**, 75 (2022)